CHAPTER III

PREPARATION OF 4-VINYLIMIDAZOLE-CO-ACRYLIC ACID COPOLYMER AND THERMAL PERFORMANCES RELATED TO APPLICABILITY AS PEM FUEL CELLS

3.1 Abstract

A series of acrylic acid and 4-vinylimidazole copolymers for a non-hydrous proton transferring membrane used in polymer electrolyte membrane for fuel cell (PEMFC) are reported. The feed ratio of each monomer results in the variation of copolymer as evaluated by Fourier transform infrared spectroscopy (FTIR), and Nuclear magnetic resonance spectroscopy (^{1}H NMR). Differential scanning calorimeter and thermal gravimetric analyzer confirm the thermal properties of copolymer films with T_g at 105-177 °C and T_d above 230 °C. The simultaneous analysis of wide angle x-ray diffraction (WAXD) and differential scanning calorimetry (DSC) suggests the thermal performance about the decrease in domain size as a consequence of the loss of moisture content in the membrane and the increase in domain size as a consequence of chain mobility after Tg. The proton conductivities under anhydrous condition of the copolymer membranes are in the range of 10^{-2} S/cm even up to 120 °C.

Keywords: Acrylic acid; 4-Vinylimidazole; Polymer electrolyte membrane fuel cell; Anhydrous membrane system

3.2 Introduction

In current years, polymer electrolyte membrane fuel cells (PEMFCs) have attracted much attention due to potential uses as energy power for automobiles, portable appliances and devices [1-5]. For membrane, the essential part in a PEMFC, Nafion® is well-accepted as it shows the high stability to the reduction and oxidation [6]. Although, the electric conductivity of Nafion® reaches as high as 10^{-2} S/cm in its

fully hydrated state [7], we have to accept that the conductivity decreases above the water boiling temperature according to the loss of absorbed water in the membranes [1, 8-9]. In particular, the polymer electrolyte membranes at operating temperature above 100 °C offer many advantages including the fast electrode kinetics, the high tolerance fuel impurities such as carbon monoxide [2, 8, 10-13]. As a consequence, new types of anhydrous polymer electrolytes based on simple system design and proton transfer efficiency above 100 °C are on the expectation [8]. Several anhydrous acid-based polymer membranes as another class of electrolyte membrane using some specific polymers and treating with strong acids and bases have been reported [14-22]. Heterocyclic aromatic compounds such as imidazole are known as strong proton acceptors to perform as the proton pathway through their resonance structures. In other words, the alternating protonation of two nitrogen atoms is assumed as donors and acceptors in proton transfer mechanism [23]. Previously, imidazole compounds blends with Nafion® and sulfonated polyether ether ketone (PEEK) were reported for conductivity improvement above 100 °C [9, 24].

Bozkurt et al. reported poly (4-vinylimidazole) (P-4VI) and H_3PO_4 with the proton conductivity of 10^{-3} S/cm at ambient temperature [25]. Pu *et al.* indicated that xH_2SO_4 (x=1) enhanced the conductivity of P-4VI than that of xH_3PO_4 [26]. Other heterocyclic molecules, such as imidazole, pyrazole, and 1-methylimidazole into poly (vinylphosphonic acid) were also reported. Among those, a significant proton conductivity 10^{-3} S/cm at 150 °C under anhydrous state was achieved in the case of poly (vinylphosphonic acid) blend with imidazole for 89 mol% [27]. Bozkurt *et al.* also reported about the anhydrous proton conducting polymer electrolytes by entrapping imidazole in polyacrylic acid. The transparent films obtained were thermally stable up to 200 °C. By increasing imidazole content, the glass transition temperature was found to decrease whereas the conductivity was found to increase (10^{-3} S/cm at 120 °C) [28]. Those approaches were to accelerate proton conductivities under an anhydrous condition using protic amphoteric materials with large self-dissociation [23]. The proton conductivities enhanced by immobilizing imidazole molecules into polymeric chain are yet to be developed [29, 30]. Recent attempt is, for example, the copolymerization of vinylphosphonic acid and 4-

vinylimidazole. This 'water free' copolymer membrane was stable up to 200 °C; however, the DC conductivities of the dry copolymers were between 10^{-6} and 10^{-12} S/cm [31]. Although, vinylphosphonic acid showed a favorable hopping mechanism, other proton donating groups, especially acrylic acid might be a good candidate in producing competitive copolymer in term of price. In this work, we consider copolymer (see Scheme 3.1) consisting of vinylimidazole unit having an imidazole group as a proton transferring part and acrylic acid unit as a proton providing part in the proton hopping mechanism. As thermal performance of the membrane is important in term of operating temperature range of PEMFC, we focus on the thermal properties and the structural changes related to the temperature and the consequent proton conductivity.

Scheme 3.1 Preparation of acrylic acid and 4–vinylimidazole copolymer

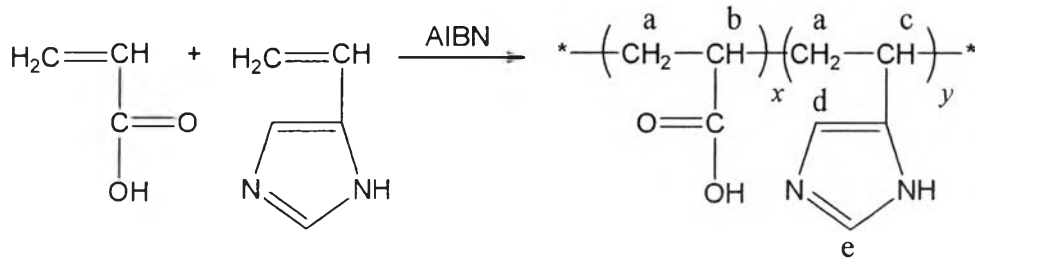

Acrylic acid 4-Vinylimidazole Poly(acrylic acid)-co-4-Vinylimidazole

1 **2** **3**

3.3 Experimental Section

3.3.1 Chemicals

Urocanic acid and 2, 2'-azobisisobutyronitrile were purchased from Sigma Aldrich (USA.). Methanol and acetone were obtained from Lab-Scan (Ireland). Acrylic acid and hydrochloric acid were purchased from Fluka Chemicals (Buchs, Switzerland). All chemicals were AR grade and used without further purification except acrylic acid.

3.3.2 Measurements

FTIR spectra were obtained from a Thermo Nicolet Nexus 670 with 32 scans at a resolution of 2 cm^{-1}. A frequency of 400-4000 cm^{-1} was observed by using deuterated triglycerinesulfate detector (DTGS) with specific detectivity, D*, of 1 x $10^9 cm \cdot Hz^{1/2} \cdot w^{-1}$. ^{1}H-NMR spectra were recorded using a Varian Mercury-400BB spectrometer. Thermal analysis was investigated by a TGA 2950 Dupont. Samples were heated to 800 °C at a heating rate 10 °C min^{-1} under nitrogen or air at a flow rate 20 ml min^{-1}. DSC was carried out at the temperature range of -70-500 °C using a DSC Q1000 series with a heat-cool-heat cycle program and heating rate 2 °C* min^{-1} (for powder) and 10 °C* min^{-1} (for film). All data were collected in the second heating cycle in order to obtain reproducible analysis. WAXD patterns were analyzed by using Rigaku Spectrometer (CuK_α) with D/MAX RINT -2000. Powder samples were adhered onto a glass slide and measured at 2θ angles between 3° and 40° in steps of 0.02° with a scan speed of 0.1 °C/min. Temperature-dependent diffraction pattern of films were measured by using simultaneous WAXD and DSC Rigaku/MSC accessories at 2θ between 3° and 40° in steps of 0.02° with scan speed 1 °C/min. Proton conductivity was measured by impedance spectroscopy with a Zahner IM6 Impedance spectrometer.

3.3.3 Procedures

3.3.3.1 Preparation of 4-vinylimidazole

Anhydrous urocanic acid (1.0 g, 0.0072 mole) was distilled in vacuo at 230 °C under pressure 35 torr. The thus-obtained colorless syrup (0.26 g) obtained was kept under nitrogen atmosphere until use. [32]

FTIR (KBr, cm^{-1}): 3200-2300 (s,br, N-H), 1643 (m, C=C), 988 (s, C-H), 939 (vs, CH_2); ^{1}H-NMR (400 MHz, $CDCl_3$, ppm): 7.64 (1H, s, N=CH), 6.95 (1H, s, N-CH), 6.56 (1H, q, =C-H), 5.64 (1H, d, =C-H), 5.13 (1H, d, =C-H).

3.3.3.2 Purification of acrylic acid

Acrylic acid (5.255 g, 0.0730 mole) was distilled under vacuo at a pressure 41-45 torr. At 120 °C, acrylic acid vapor was crystallized in the receiver. The purified **1** was kept under N_2.

3.3.3.3 Synthesis of copolymers of acrylic acid and 4-vinylimidazole

The reaction was carried out as reported in previous papers [32, 33]. In brief, 4-Vinylimidazole (0.2 g, 0.0021 mole) and freshly distilled acrylic acid (0.8 g, 0.0111 mole) were dissolved with AIBN (0.1 mole %) in methanol (5 mL). After degassing and flushing with nitrogen, the flask was sealed and heated to 70-75 °C. The white suspension was obtained after 15 minutes. The suspension was washed thoroughly several times with acetone-methanol and the white precipitate was collected. A series of reactions using different molar ratios of acrylic acid and 4-vinylimidazole, i.e., 1:4, 1:1, 4:1, and 19:1 were carried out similarly.

85% yield (1:4 of acrylic acid and 4-vinylimidazole), 69% yield (1:1), 66% yield (4:1), 62% yield; FTIR (film, cm^{-1}): 3550-3300 (br, O-H), 3200-2300 (s, br, N-H), 1712 (s, C=O), 1630 (s, COO^-), 1445 (m, CH_2), 1175 (s, C-O); ^{1}H-NMR (400 MHz, 1%DCl in D_2O, ppm): 8.2-8.6 (1H, m, 2-H in imidazole),7.2-6.6 (1H, m, 4-H in imidazole), 2-3 (1H, m, -CH), 1-2 (2H, m, $-CH_2$); *Anal.* Calcd for $C_{23}H_{28}O_2N_8$: C, 61.6; H, 6.25; and N, 25. Found: C, 52.39; H, 6.48; and N, 20.09. *Anal.* Calcd for $C_8H_{10}O_2N_2$: C, 57.8; H, 6.02; and N, 16.86. Found: C, 50.08; H, 6.34; and N, 14.4. *Anal* calcd for $C_{17}H_{22}O_8N_2$: C, 53.4; H, 5.76; and N, 7.33. Found: C, 49.47; H, 5.9; and N, 7.76. *Anal.* Calcd for $C_{62}H_{82}O_{38}N_2$: C, 44.82; H, 4.94; and N, 1.68. Found: C, 46.99; H, 5.99; and N, 1.6.

3.3.3.4 Membrane preparation

Copolymer membranes were prepared by casting the 5 wt% copolymer samples in 1% hydrochloric acid/water (v/v) solution on smooth PTFE plate (3 cm×3 cm). The cast solution (10 mL) was evaporated at 50 °C for 48 h to obtain transparent thin films were obtained with 110 μm thickness.

3.3.3.5 Proton conductivity measurement

Membranes were sandwiched between gas diffusion electrodes (ELAT® containing 0.25 mg/cm^2 Pt loading) using porous stainless steel discs. The conductivity of membranes was carried out as a function of temperature (from 40 to 120 °C) without humidity in the frequency ranges 10 Hz-1MHz at the signal amplitude ≤100 mV. The impedance measurement was calibrated on the basis of the contribution of the empty and short-circuited cell. The membrane resistance was obtained from the extrapolation of the real axis on the high frequency part. All conductivity measurements were carried out after the conductivity reaching a constant value at least 3 h. The proton conductivity was recorded as the impedance value at zero phase angles.

3.4 Results and Discussion

It is important to note that urocanic acid could not be used directly for copolymerization due to the steric effects of 1, 2-disbstituted alkenes [34]. In order to obtain 4(5)-vinylimidazole, urocanic acid was decarboxylated by vacuum distillation. The peaks referring to 4(5)-vinylimidazole were clarified as follows, 789 cm^{-1} (five membered heterocyclic), 3130 cm^{-1} and 1520 cm^{-1} (stretching and bending vibrations of secondary aromatic amine) and broad peaks at 2800-2600 cm^{-1} (N-H---N).

^{1}H-NMR was also used to confirm monomer structure of 4(5)-vinylimidazole. Urocanic shows the chemical shift at 3-4 ppm (-OH) and 6.41 ppm (CH=) whereas the chemical shifts referring to 4(5)-vinylimidazole are two singlet peaks at 7.067 and 7.647 ppm for N-CH and N=CH protons (imidazole), respectively. The methylene (CH_2=) and methine (=CH) protons of 4(5)-vinylimidazole appears 5.2, 5.7, and 6.6 ppm.

3. 4.1 Copolymerization

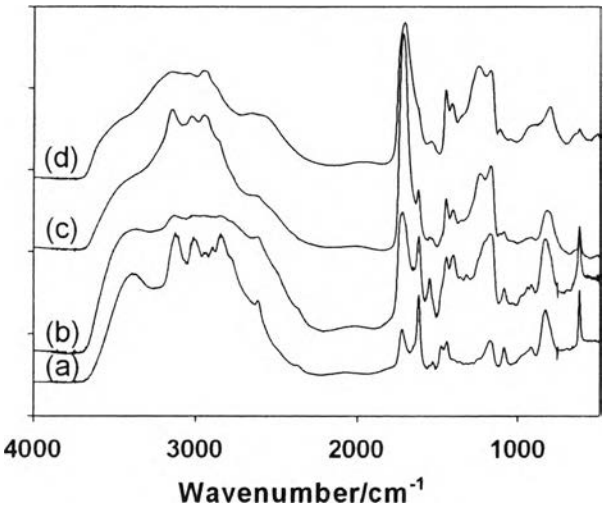

Figure 3.1 FT-IR spectra of the compound obtained from the reaction of acrylic acid and 4(5)-vinylimidazole: (a) **M1**, (b) **M2**, (c) **M3**, and (d) **M4**.

Copolymers of acrylic acid and 4(5)-vinylimidazole were reported by Overberger and Vorcheimer with an objective of polymeric model enzyme systems [12]. The reaction of 4(5)-vinylimidazole and acrylic acid was carried out following this literature with various monomer feed ratios. After the reaction, the strong C=O peak at 1712 cm^{-1} increased in intensity as the acrylic acid mole ratio was increased (see Figure 3.1 a-d). In addition, the peaks at 1250 cm^{-1} belonging to the in plane deformation of C-O-H and at 1180 cm^{-1} to –(C-O) H stretching of acrylic acid can be observed. It should be noted that **M1-M4** have both acidic and basic units which can conduct protons over the heterocyclic units based on structural diffusion mechanism (Grotthus mechanism). As free carboxyl group tends to broaden, the hydrogen-bonding peaks of CO_2^- at 1625 and 1553 cm^{-1} are increased. In our case, the broadening of the C=O bond implies the hydrogen bond between acrylic acid and imidazole groups. N-H stretching increased as the 4-VIm content increased. It could be explained that proton exchange reactions are occurred by the hydrogen-bonded network of carboxylic acid and imidazole molecules [36].

Figure 3.2 shows ^{1}H-NMR spectra of acrylic acid and 4(5)-vinylimidazole. The chemical shifts at 7-8 ppm are assigned to imidazole ring. The peaks at 1-3 ppm are attributed to the methylene and methine protons. This suggests the chemical structure of the copolymer between acrylic acid and 4(5)-vinylimidazole. In order to quantify the copolymer content, ^{1}H-NMR spectra were carried out. As shown in Scheme 3.1, the copolymer protons were assumed to be a, b and c. Based on the proton intensity of imidazole and polymer backbone, 4(5)-vinylimidazole content was calculated and summarized in Table 3.1. The *y* contents in percent for **M1**, **M2**, **M3**, and **M4** were then found to be 66.6, 64.5, 28.57, and 4.16, respectively.

$$\% \text{ 4(5)-Vinylimidazole content in the copolymers} = (I_{H\text{-}d}/(I_{H\text{-}a}/2)) \times 100$$

Table 3.1 Acrylic acid (AA) (*x*) and 4(5)-vinylimidazole (4-VIm) (*y*) monomers with the 4(5)-vinylimidazole content of the copolymers

Membrane	Feed ratio (mol) AA/ 4-VIm (*x*:*y*)	4-VIm content (y%) by ^{1}H-NMR
M1	1:4	66.6
M2	1:1	64.51
M3	4:1	28.57
M4	19:1	4.16

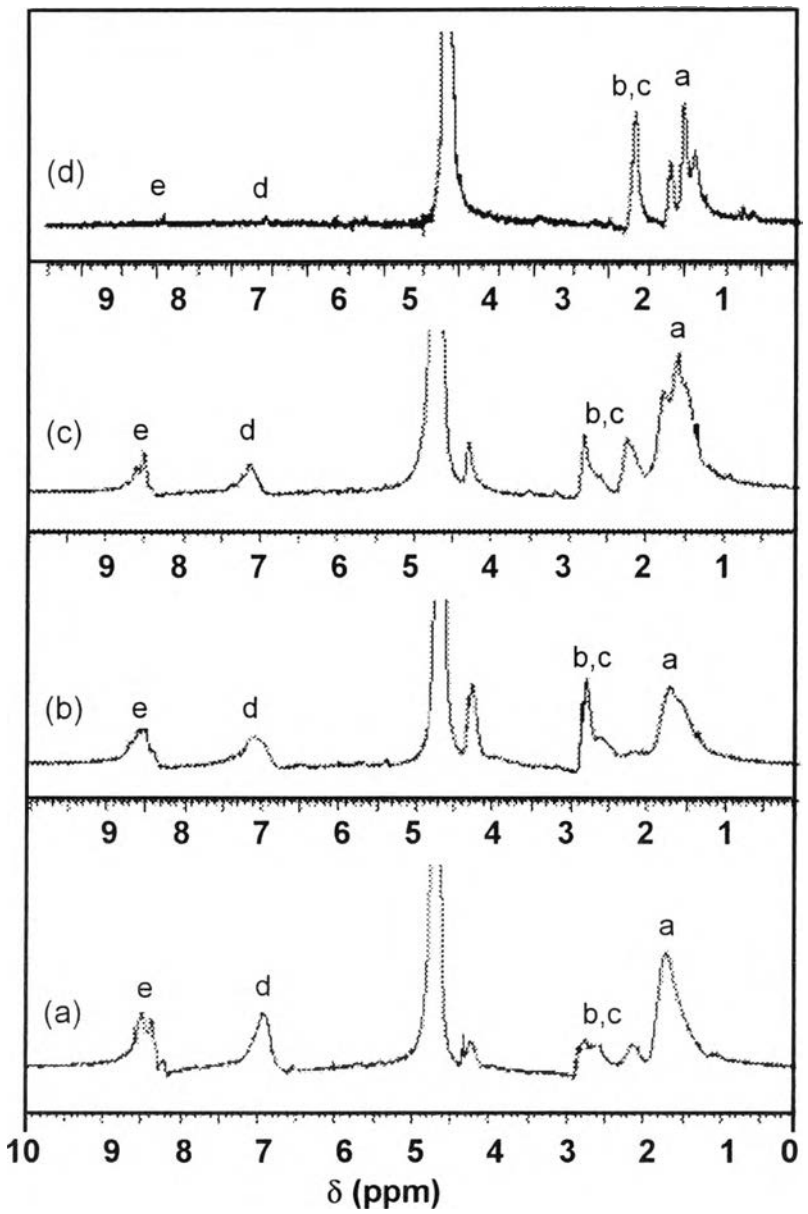

Figure 3.2 ^{1}H-NMR spectra of copolymers of acrylic acid and 4(5)-vinylimidazole: (a) **M1**, (b) **M2**, (c) **M3**, and (d) **M4**.

In the past, monomer reactivity ratios of acrylic acid (r_1) and (r_2) 4(5)-vinylimidazole were determined as $r_1 = 0.06\pm0.01$ and $r_2 = 0.11\pm0.04$ and $r_1r_2 = 0.0066$. This means that copolymerization between these two monomers gives an alternating copolymer [33, 35]. Therefore, in the case of **M2**, the found ratio is closed to that of the feed ratio; we suspect that the copolymer is an alternating one.

When the amount of 4(5)-vinylimidazole is very low, i.e. **M4**, the alternating copolymer might be difficult to form as seen in the copolymer content evaluated by ^{1}H-NMR.

3.4.2 Thermal stability

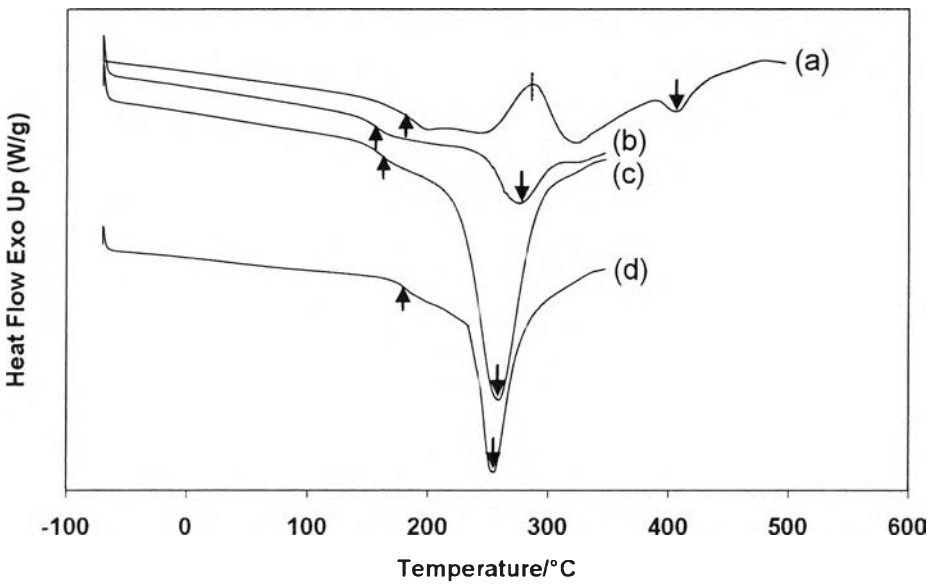

Figure 3.3 DSC thermograms of copolymer powders of acrylic acid and 4(5)-vinylimidazole: (a) **M1**, (b) **M2**, (c) **M3**, and (d) **M4,** arrow up for Tg and arrow down for Tm.

Characteristic DSC curves of nature copolymers are shown in Figure 3.3. The copolymer powders exhibit the glass transition temperature at 190.6 °C, 155.8 °C, 162.5 °C, and 178.4 °C, for the sample **M1**, **M2**, **M3**, and **M4**, respectively. It is important to note that **M1** gives both the crystallization and melting temperatures at 287 °C and 407 °C whereas **M2**, **M3**, and **M4** give only the melting temperature at 273 °C, 258 °C, and 255 °C, respectively. Those Tc and Tm are above the degradation temperature of the samples which is also detected by TGA. It should be noted that the copolymers obtained couldn't dissolve in most common solvents. When **M1**-**M4** were cast as membranes by using 1%HCl/H_2O, their glass transition temperatures were shifted to lower temperature at 177.2 °C (**M1**), 146.1 °C (**M2**),

135.8 °C (**M3**), and 105.9 °C (**M4**) (see Figure 3.4). The lowering of Tg implies that the membrane casting might initiate amorphous morphology which the inter- and intra-molecular hydrogen bond of the copolymers were significantly decreased.

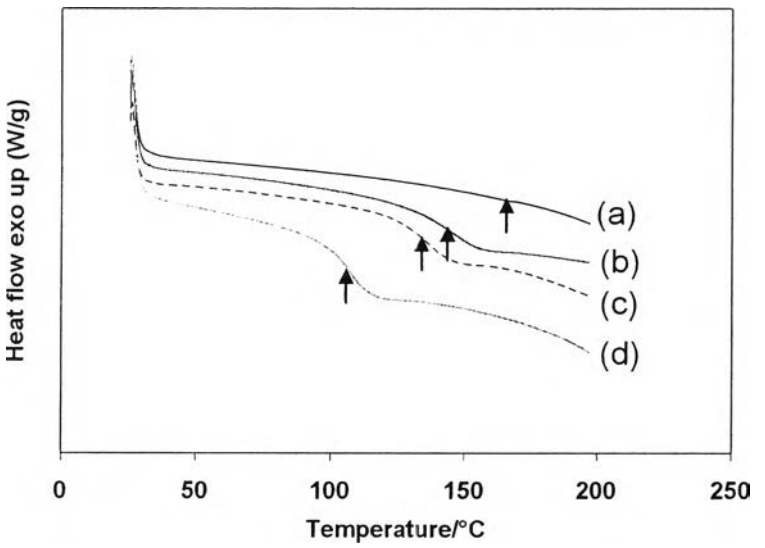

Figure 3.4 DSC thermograms of copolymer films of acrylic acid and 4(5)-vinylimidazole: (a) **M1**, (b) **M2**, (c) **M3**, and (d) **M4,** arrow up for Tg.

Thermogravimetric analysis was applied to observe the thermal stability of the copolymer film obtained. The TGA studies under the air (or O_2) give the information about the thermal degradation via oxidation, whereas the ones under the N_2 demonstrate the chain degradation without oxidation. Either the case under the air or nitrogen, a significant 10-15% weight loss from 50-150 °C is identified (see Figure 3.5). This suggests the physically bound water in the product which can be detected by the first heating cycle of DSC. The degradation region at 150-200 °C was assigned to the water release of the non-cyclic anhydrides formation in the acrylic acid repeat unit [37]. Moreover, the copolymer also shows the degradation starting from 230 to 380 °C. This might be due to the degradation of carboxylic acid pendant group [31]. The weight loss from 380-500 °C might be owing to the imidazole pendant group [25]. The complete degradation in air after 650 °C belongs to the C-C bond cleavage of polymer backbone.

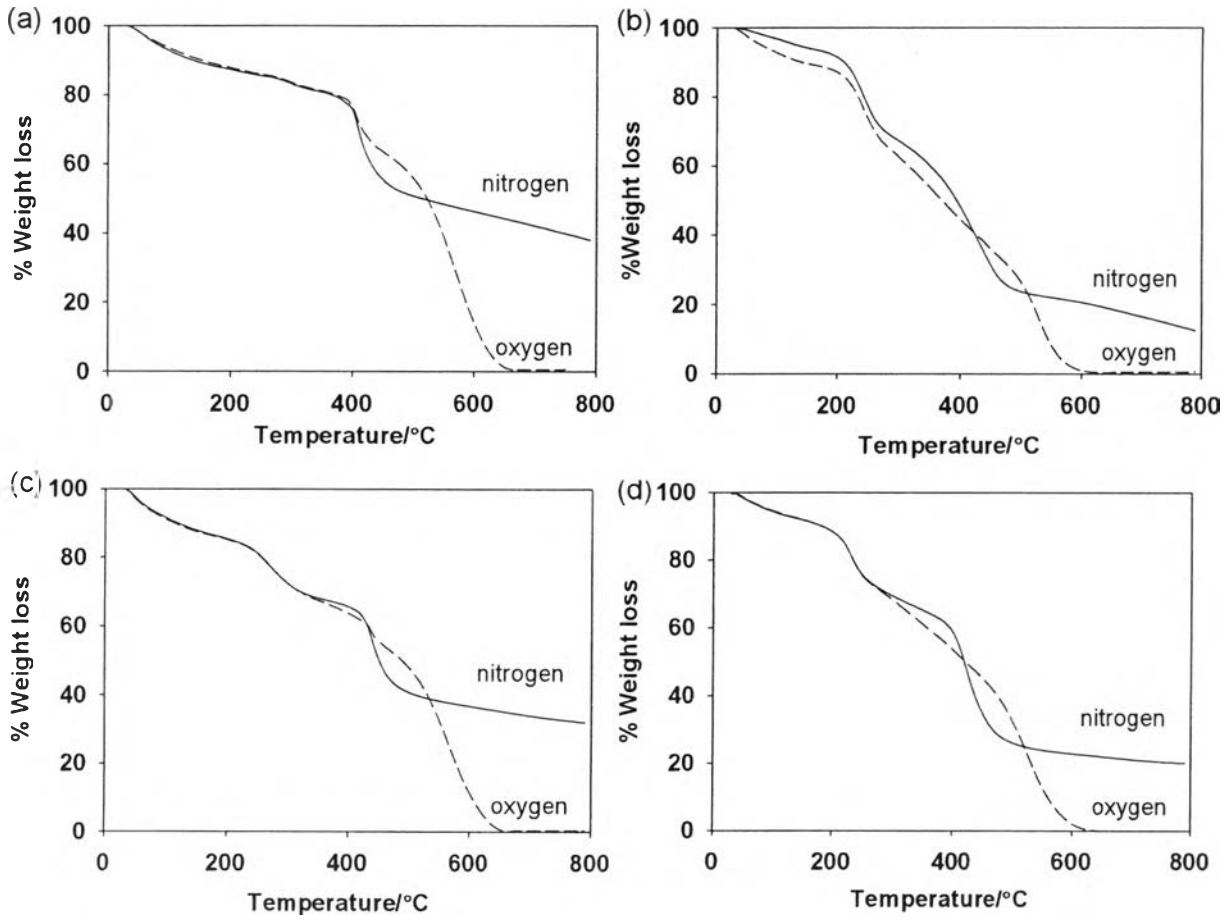

Figure 3.5 TGA thermograms of copolymer films of acrylic acid and 4(5)-vinylimidazole: (a) **M1**, (b) **M2**, (c) **M3**, and (d) **M4**.

3.4.3 Packing structure and its temperature dependence

In practical, the membrane has to be used in the temperature range 80-120 °C. In order to identify how the copolymer content and the temperature affects the packing structure, especially in the condition where water excluded, the temperature dependence diffraction patterns were measured by a simultaneous WAXD and DSC system.

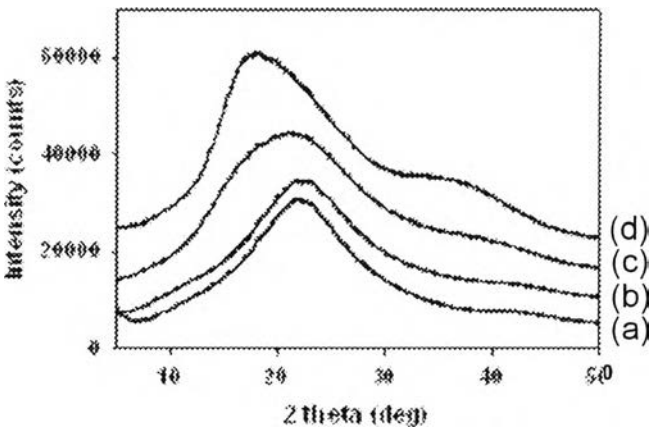

Figure 3.6 WAXD patterns of the copolymers: (a) **M1**, (b) **M2**, (c) **M3**, and (d) **M4**.

Figure 3.6 shows all the membranes give the broad peak at room temperature of which the d-spacing is 4.05, 4.15, 4.38, and 4.91 Å for **M1**, **M2**, **M3**, and **M4** respectively. As acrylic acid copolymer or homopolymer content is increased, the d-spacing increases to higher angle side. The significant loose packing structure of the membrane **M4** as compared to the other membranes can also be confirmed from the Tg (see Figure 3.4) [38].

Figure 3.7 shows important information about the increases in d-spacing upon the thermal vibration. The d-spacing of the membrane **M4** is in the range of 5.2-5.4 Å which is the highest as compared to the the other membranes. Domain size was calculated from area under peak divided by FWHM. The domain of crystallite size informs the packing structure changes during thermal vibration. The domain sizes are decreased gradually and at a certain temperature, or so-called the transition temperature, they start increasing again. The decrease in domain size is relevant to the water release temperature as combined with the DSC and TGA results (see Figure 3.5). It is significantly to note that the transition point of domain size in each membrane is close to its Tg. The changes in domain size imply that the loss of the absorbed water initiates the decrease in domain size whereas the highly free rotation after Tg induce the increase in domain size.

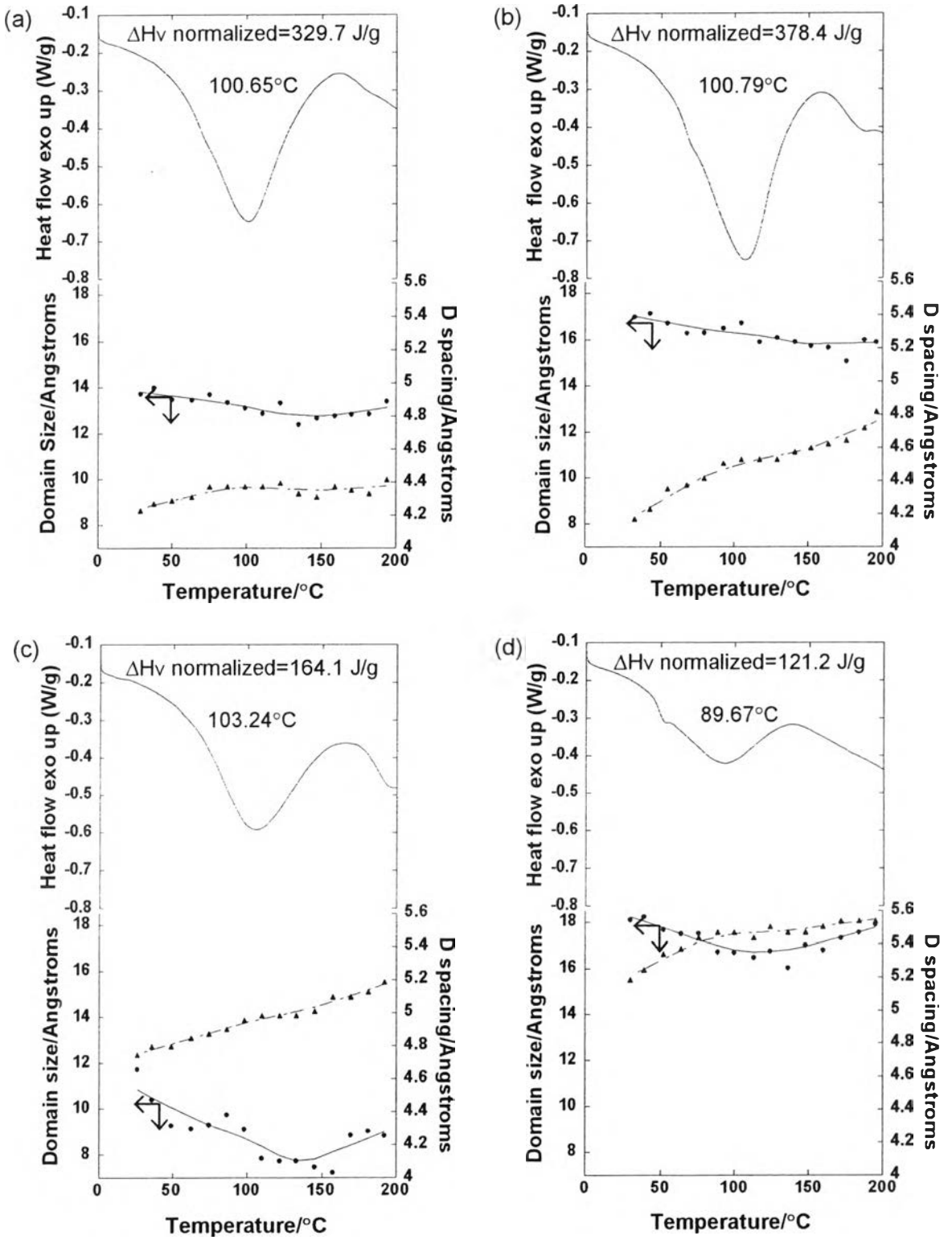

Figure 3.7 WAXD with high temperature dependency and DSC first heating cycle of the copolymers: (a) **M1**, (b) **M2**, (c) **M3**, (d) **M4**.

3.4.4 Proton conductivity

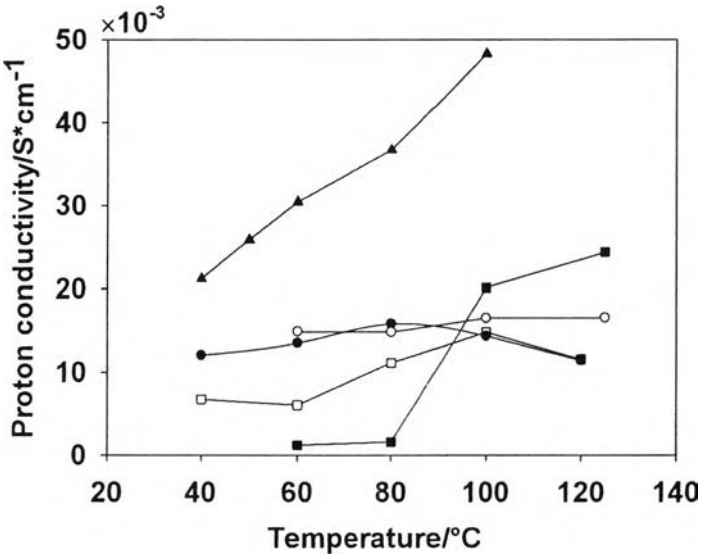

Figure 3.8 Proton conductivities in anhydrous system of copolymers: (■) **M1**, (□) **M2**, (●) **M3**, (○) **M4**, and (▲) Nafion® 115.

As the membranes were designed for the proton conductivity based on the proton hopping mechanism in between the imidazole molecules, the proton conductivity measurement was carried out without any additional moisture purging in the system. In addition, the membranes were tested without additional heat or acid treatment. As the Tg for all the membranes are much higher than the temperature used in PEMFC (see Figure 3.4), the consideration of the limitation of the temperature used for PEMFC (~120 °C) can be neglected. Figure 3.8 shows all types of the synthesized membranes including 'fully hydrated and acid treated Nafion®'. In the case of Nafion®, the proton conductivity is in the range of 20-50 mS/cm. The conductivity increases with 4(5)-vinylimidazole content, resulting in the conductivity as high as 2.4×10^{-2} S/cm under anhydrous system. In other words, the proton conductivities are stable at 10^{-2} S/cm from 60 to 125 °C. In the past it was reported that the blends of polyacrylic acid and imidazole gave the conductivity 10^{-3} S/cm at 120 °C [28]. This implies that the acrylic acid and imidazole functional groups play an important role in inducing the proton conductivity under anhydrous atmosphere. It can be seen that the membrane **M1** shows a significant increase after 80 °C. At

present stage; we suspect that as the membrane **M1** contains less acid proton content (as a consequence of less acrylic acid copolymer content (see Table 3.1), the conductivity at initial stage (60-80 °C) is rather low as compared to the other membranes. However, after 80 °C, the rich of imidazole group may function in an effective proton transferring among the membrane. Further confirmation is carrying out.

3.5 Conclusions

A series of poly (AA-co-4-VIm) were prepared and aimed for the proton conductivity via the acrylic acid and imidazole groups. The copolymers were found to be mainly the alternating copolymer formation followed by the mixtures of homopolymer and copolymers when the feed ratios of acrylic acid increased. The studies on thermal properties indicated that the Tg values of the copolymers (~155-190 °C) were shifted down significantly (~105-177 °C) after casting the membrane using acid solvent. The simultaneous WAXD-DSC showed how d-spacing increased as a consequence of thermal vibration. At that time, the domain sizes showed the decrease for the loss of moisture and the increase for chain vibration after the Tg. As the Tg for all the membranes were much higher than the temperature used in PEMFC, the proton conductivity could be easily identified based on the copolymer content from room temperature to above 120 °C. All the membranes showed the conductivity at 10^{-2} S/cm whereas the membrane with high imidazole content showed a significant increase in conductivity at the temperature above 80 °C. At present, we are investigating the mechanism of the proton conductivity via imidazole and acrylic acid groups by using temperature dependent and simultaneous analyses, such as WAXD-DSC, SAXS-Raman, etc including the simulation based on the molecular modeling.

3.6 Acknowledgements

The authors gratefully acknowledge the research fund from Joint Research Program between the National Research Council of Thailand and Japan Society for

the Promotion of Science (NRCT-JSPS). We would like to thank National Metal and Materials Center-Chiang Mai University (MTEC-CMU) for the scholarship, and Fuel Cell Research Unit, Chulalongkorn University for the support.

3.7 References and Notes

[1] Carrette L, Friedrich K, Stimming U. Fuel Cells 2001;1:5-39.

[2] Rikukawa M, Sanui K. Prog Polym Sci 2000;25:1463.

[3] Smitha B, Sridhar S, Khan AA. J Membr Sci 2005;259:10.

[4] Wieser C. Fuel Cells 2004;4:245.

[5] Haile SM. Acta Materialia 2003;51:5981.

[6] Wakizoe M, Velev OA, Srinivasan S. Electrochimica Acta 1995;40:335.

[7] Kreuer KD. Chem Mater 1996;8:610.

[8] Qingfeng Li, Ronghuan He, Jens Oluf Jensen, and Niels J.Bjerrum. Chem Mater 2003;15:4896.

[9] Yang C, Costamagna P, Srinivasan S, Benziger J, Bocarsly AB. J Power Sources 2001;103:1.

[10] Kerres JA. J Membr Sci 2001;185:3.

[11] Kreuer KD. J Membr Sci 2001;185:29.

[12] Kreuer KD. Chemphyschem 2002;3:771.

[13] Schuster MFH, Meyer WH, Schuster M, Kreuer KD. Chem Mater 2004;16:329.

[14] Donoso P, Gorecki W, Berthier C, Defendini F, Poinsignon C, Armand MB. Solid State Ionics 1988;28-30:969.

[15] Petty-Weeks S, Zupancic JJ, Swedo JR. Solid State Ionics 1988;31:117.

[16] Rogriguez D, Jegat T, Trinquet O, Grondin J, Lassegues JC. Solid State Ionics 1993;61:195.

[17] Bozkurt A, Meyer WH. J Polym Sci Part B 2001;39:1987.

[18] Mecerreyes D, Grande H, Miguel O, Ochoteco, Marcilla R, Cantero I. Chem Mater 2004;16:604.

[19] Tanaka R,Yamamoto H, Shono A, Kubo K, Sakurai M. Electrochim Acta 2000;45:1385.

[20] Grondin J, Rodriguez D, Lassegues JC. Solid State Ionics 1995;77:70.

[21] Senadeera GKR, Careem MA, Skaarup S, West K. Solid State Ionics 1996;85:37.

[22] Bozkurt A, Ise M, Kreuer KD, Meyer WH, Wegner WH, Wegner G. Solid State Ionics 1999;125:225.

[23] Munch W, Kreuer KD, Silvestri W, Maier J, Seifert G. Solid State Ionics 2001;145:437.

[24] Kreuer KD, Fuchs A, Ise M, Spaeth M, Maier J. Electrochimica Acta 1998;43:1281.

[25] Bozkurt A, Meyer WH. Solid State Ionics 2001;138:259.

[26] Pu H, Meyer WH, Wegner G. Macromol Chem Phys 2001;202:1478.

[27] Yamada M, Honma I. Polymer 2005;46:2986.

[28] Munch W, Kreuer KD, Silvestri W, Maier J, Seifert G. Solid State Ionics 2001;145:437.

[29] Kreuer KD. Solid State Ionics 1997;94:55.

[30] Schuter M, Meyer WH, Wegner G, Herz HG, Ise M, Kreuer KD, Maier J. Solid State Ionics 2001;145:85.

[31] Bozkurt A, Meyer WH, Gutmann J, Wegner G. Solid State Ionics 2003;164:169.

[32] Overberger CG, Vorchheimer N. J Am Chem Soc 1963;85:951.

[33] Overberger CG, Maki H. Macromolecules 1970;3:214.

[34] Krzysztof Matyjaszewski and Thomas P. Davis. Handbook of radical polymerization. John Wiley and Sons, Inc., 2002. pp. 3.

[35] Kreuer KD, Paddison SJ, Spohr E, and Schuster M. Chem Rev 2004;104:4637-4678.

[36] Manas Chanda. Advanced polymer chemistry: a problem solving guide. Marcel Dekker, Inc. pp 587.

[37] Stanislav Dubinsky, Gideon S Grader, Gennady E Shter, and Michael Silverstein. Polym Degrad Stab 2004;86:171-178.

[38] Hatakeyama T, Hatakeyama K, Hatakeyama H. Themochimica Acta 1988;123:153.